ELSEVIER

Chemical Engineering Journal 68 (1997) 123–130

Chemical Engineering Journal

Crystallization of calcium sulphate hemihydrate in concentrated phosphoric acid solutions

M. El Moussaouiti [a], R. Boistelle [a,*], A. Bouhaouss [b], J.P. Klein [c]

[a] *Centre de Recherche sur les Mécanismes de la Croissance Cristalline,[1] CRMC2-CNRS, Campus de Luminy, case 913, F-13288 Marseille Cedex 09, France*

[b] *Laboratoire de Chimie-Physique Générale, Université Mohammed V, Faculté des Sciences, Av. Ibn Battouta, Rabat, Morocco*

[c] *Laboratoire d'Automatique et de Génie des Procédés, Université Lyon I et CPE Lyon, 43 Bd du 11 Novembre 1918, F-69622 Villeurbanne Cedex, France*

Received 20 May 1996; accepted 28 May 1997

Abstract

We aim to show the existence of agglomeration by measuring and modelling secondary nucleation and crystal growth rates of calcium sulphate hemihydrate, $CaSO_4$–0.5 H_2O, in concentrated phosphoric acid solutions. Using a batch crystallizer we measured the evolution of the population density as a function of supersaturation, H_2SO_4 excess and stirring rates. All experiments were carried out at 90 °C in solutions at 40 wt.% of P_2O_5, simulating the usual conditions for crystallizing hemihydrate in the industrial processes of phosphoric acid production.

Nucleation and growth rates were calculated from the population number densities, using the moments analysis method. A model is presented for describing the crystallization process of hemihydrate. It is shown that secondary nucleation and growth rates are quadratic functions of supersaturation. H_2SO_4 concentrations affect supersaturation but at the same supersaturation the growth rates are not significantly different. Nucleation is independent of the stirring rate, whereas growth rates are slightly affected for stirring rates up to 500 rpm. Taking agglomeration into account, the moments method fits very well the experimental data. © 1997 Elsevier Science S.A.

Keywords: Calcium sulphate hemihydrate; Crystallization; Secondary nucleation

1. Introduction

Wet processes, using digestion of phosphate rocks by sulphuric acid, are the most common processes used to produce phosphoric acid. The overall and simplified reaction between monocalcic phosphate and sulphuric acid [1,2] can be written as:

$$CaH_4(PO_4)_2 + H_2SO_4 + xH_2O \rightarrow CaSO_4xH_2O + 2H_3PO_4$$

where x is 0 for calcium sulphate anhydrate, 0.5 for hemihydrate and 2 for dihydrate, i.e. gypsum. The nature of the solid phase that forms first [3] depends on the conditions under which the reaction takes place (Fig. 1). Metastable and stable phases may occur separately, simultaneously or successively depending on the crystallization kinetics. Hemihydrate crystallization is an important stage in the industrial process of phosphoric acid production, whether hemihydrate is the final by-product or the initial solid phase intended to be recrystallized into gypsum [4–7]. The so-called hemihydrate process has several advantages with respect to the dihydrate process:

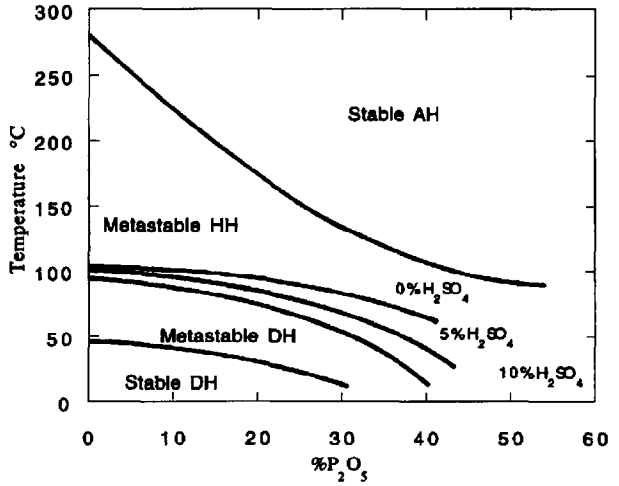

Fig. 1. Equilibrium diagram for the system $CaSO_4$–P_2O_5–H_2O after Dahlgren [3]: anhydrate (AH), hemihydrate (HH) and dihydrate (DH).

- the phosphate ore is more easily solubilized
- the phosphoric acid production is higher
- the hemihydrate is relatively stable and does not transform too rapidly into gypsum.

Amin and Larson [8] were the first to study calcium sulphate hemihydrate crystallization in phosphoric acid solu-

* Corresponding author. Tel.: (33) 04 91 17 28 11; fax: (33) 04 91 41 89 16; e-mail: Boistelle@crmc2.univ-mrs.fr

[1] Associated with Univ. Aix-Marseille II and III.

PII S1385-8947(97)00116-2

tions under the conditions of an industrial hemihydrate process. The experimental data were fitted using the concept of population balance, but without taking crystal agglomeration into account. Gioia et al. [9] described a model for continuous crystallization of hemihydrate grounded on the data of Amin and Larson. However, agglomeration always takes place as soon as the P_2O_5 concentration in the solution exceeds about 40 wt.%. Pozin et al. [2] were the first to point out the existence of agglomeration in pure solutions, a phenomenon they called coagulation. Later on, Davenport et al. [10] reported the presence of hemihydrate agglomerates in industrial liquors at 40% P_2O_5 and H_2SO_4/CaO ratios ranging from 0.92 to 1.08 (weight ratios). The agglomerate size was about 100 μm. Torocheshnikov and Petrovlovskii [4] qualitatively studied the influence of some parameters on the stability of the agglomerates formed during the recrystallization process of dihydrate into hemihydrate. In phosphoric acid solutions, without impurities, the agglomerate size was about 30 μm. Finally, van der Sluis et al. [11] studied hemihydrate agglomeration, also in pure solutions, as a function of H_2SO_4 and H_3PO_4 concentrations. It was pointed out that agglomeration occurs at 40% P_2O_5, even with increasing H_2SO_4 concentration. Concerning nucleation and growth rates, it must be emphasized that they are very difficult to determine, because nucleation, growth and agglomeration occur almost simultaneously. In other systems, as potassium sulphate growing from aqueous solutions [12], only agglomeration and ripening were considered, because supersaturation was kept at a very low level. However, in the case of adipic acid studied by Marchal et al. [13], agglomeration also occurred during nucleation and growth, and was taken into account in the crystallization model.

2. Experimental

2.1. Chemicals

In all experiments we used pure chemicals (trade mark Prolabo): aqueous solutions of H_3PO_4 (84%) and H_2SO_4 (95%), solid $CaCO_3$. The percentages given here, and in the following pages, are expressed in weight per cent. The stock solutions (P) of monocalcic phosphate were prepared by dissolution of 35.7 g $CaCO_3$ in 964.3 g phosphoric acid at 40% P_2O_5. This corresponds to a solution of 2% CaO. The solution at 40% P_2O_5 is a solution containing 55.2% H_3PO_4. We always use P_2O_5 and CaO concentrations which are traditionally encountered in the industry of phosphoric acid. The monocalcic phosphate formation corresponds to the reaction:

$$CaCO_3 + 2H_3PO_4 \rightarrow Ca(H_2PO_4)_2 + H_2O + CO_2$$

The solutions were stored and stirred at least overnight, in order to fully remove CO_2. Sulpho-phosphoric stock solutions (A) were prepared by adding 36.82 g sulphuric acid to 963.18 g phosphoric acid at 40% P_2O_5. The molarity in H_2SO_4 of the A solutions was now the same as the molarity in CaO of the P solutions. For a certain mixture P + A, the H_2SO_4 excesses were calculated as weight per cent with respect to the mixture P + A. H_2SO_4 was added to A before mixing P and A.

2.2. Experimental procedure

The experiments were carried out in a double jacketed glass crystallizer, the volume of which was 2 l, equipped with a draft tube, three wall baffles to prevent the solution from rotating, and a stirrer in Hastolloy G30 especially designed (trade mark Mixel, model TT, diameter 70 mm) for obtaining a homogeneous suspension even at the lowest stirring rate being used. The crystallizer was thermostatically regulated by circulating water through the double walls.

To carry out an experiment, the crystallizer was first filled with the proper mass of solution P (about 1 kg) and heated up to 90 °C. The same mass of solution A, previously stored at 80 °C, was then rapidly poured, within 30 s, into solution P. Mixing the solutions brought the whole mixture to 90 °C.

The initial supersaturation $\sigma_0 = (C - C_0)/C_0$, before the occurrence of nucleation, was adjusted by changing the initial amounts of solutions A and P. C and C_0 were the actual and equilibrium concentrations of calcium. For the sake of simplicity, as solubility is small, these concentrations are expressed in mmol l^{-1}. Growth of the hemihydrate crystals was followed by regular removal of suspension volumes of 20 cm^3. A portion of each sample (6 cm^3) was filtered through a 0.2 μm cellulose filter, the supernatant being used for analysing the calcium concentration (Corning calcimeter) to follow supersaturation versus time. The other portion of the suspension was filtered through a sintered glass filter no. 4, rinsed twice with ethanol, once with acetone, and finally dried at 40 °C. As the solution composition changed due to the H_2SO_4 excesses, solubility of hemihydrate was determined at the end of each experiment, also by analysing the calcium concentration. Each experiment lasted about 2 h. The nature of the crystals was checked by X-ray diffraction to ensure that there was no transformation of hemihydrate into gypsum. The solubility data are displayed in Fig. 2 and com-

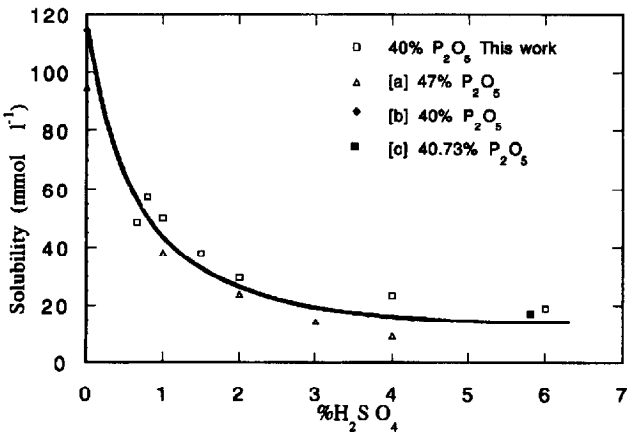

Fig. 2. Solubility of calcium sulphate hemihydrate at 90 °C in aqueous solution of phosphoric acid at 40% P_2O_5 and 90 °C, for different H_2SO_4 excesses (after (a) Jansen et al. [14], (b) Sullivan et al. [15], (c) Khan [16]).

pared to those of Jansen et al. [14], Sullivan et al. [15], and Khan [16].

To determine crystal size distributions, the crystals, dried at 40 °C, were put again in suspension, an electrolytic solution obtained by dissolution of 2% LiCl in absolute ethanol, subsequently filtered at 0.2 μm. The volume of the electrolytic solution was the same as the volume of solution in the suspension removed from the crystallizer. We aimed at exactly reproducing the population number densities existing in the crystallizer. Subsequently, 1 cm^3 of this new suspension was diluted 100 times with the electrolytic solution and analysed with an ELZONE 180 PC counter, the measurement principle of which is the same as that of the Coulter counter. The particles were counted and their sizes distributed in 128 size classes. The real size distribution, existing in the crystallizer, per unit volume of suspension, was recalculated from the counting time (10 s), the flux of suspension through the tube orifice of the counter $Q = 24$ cm^3 min^{-1}, and the dilution factor by means of

$$[N] = \frac{n \times 6}{Q} \times 100 \tag{1}$$

where $[N]$ is the number of particles per unit volume of suspension and n the number of particles counted during 10 s.

The sizes L_i, which are the equivalent diameters of the particles in the size classes i, are calculated in the treatment of the size distribution according to the expression:

$$\log(L/L_0) = 8n_i \log(1.0027) \tag{2}$$

where n_i is the number of the size class i and L_0 the smallest size detected by the counter. In our case $L_0 = 10.61$ μm for a tube orifice of 300 μm, so that the size range of the analyser is 10.61–150 μm, and log(1.0027) is the so-called interchannel. The width of a size class is $\Delta L_i = L_i - (L_{i-1})$ from which we obtain the population number densities $\Psi(L_i)$:

$$\Psi(L_i) = [N]/\Delta L_i \tag{3}$$

$\Psi(L_i)$ is the number of particles per unit volume of suspension and length in the class L_i. Once the $\Psi(L_i)$ values are known, it is possible to calculate the population volume densities $\Psi'(v_i)$, the number of particles in the class of volume v_i. Since the equivalent size measured by the ELZONE device is the diameter of a sphere of the same volume, they are calculated by

$$v_i = \frac{\pi}{6} L_i^3 \tag{4}$$

Figs. 3 and 4 give an example of a particle concentration as a function of the equivalent diameter L and a population number density as a function of the particle volume v.

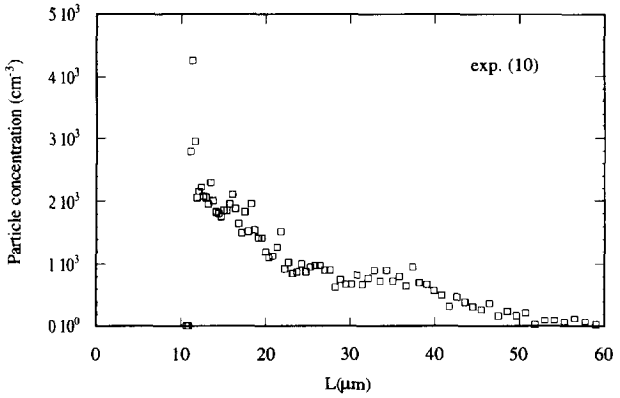

Fig. 3. Particle concentration as a function of the equivalent diameter L.

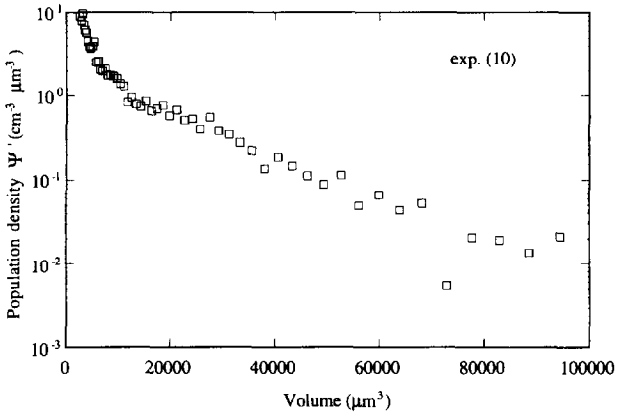

Fig. 4. Population number density in the crystallizer at time t, deduced from the data displayed in Fig. 3, vs. particle volume.

3. Theoretical considerations

3.1. Population balance

The population balance in a batch crystallizer, where the crystallizing solid does not significantly change the total volume of the suspension, may be written with respect to the volume population density function Ψ' as:

$$\frac{\partial \Psi'}{\partial t} + \frac{\partial(\Psi' G_v)}{\partial v} = B\delta(v - v^*) + r_A - r_B \tag{5}$$

where G_v is the volume growth rate dv/dt, r_A the distribution of the agglomeration rates, r_B the distribution of the breakage rates, B the nucleation rate and $\delta(v - v^*)$ the Dirac function, since v^* is the volume of the critical nuclei.

In the case of calcium sulphate hemihydrate the agglomerates formed at mean supersaturation are stable, as we will see later. There is no breakage. Accordingly, the population balance for $v \neq v^*$ (i.e. L different from the critical size L^*) is given by

$$\frac{\partial \Psi'}{\partial t} + \frac{\partial(\Psi' G_v)}{\partial v} = r_A \tag{6}$$

When agglomeration is negligible we get

$$\frac{\partial \Psi'}{\partial t} + \frac{\partial(\Psi' G_v)}{\partial L} = 0 \tag{7}$$

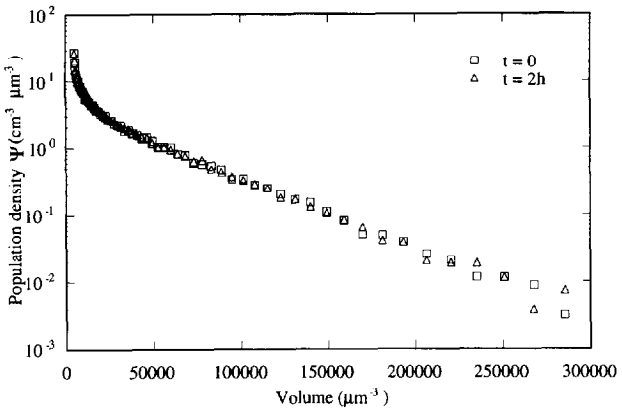

Fig. 5. Variation of the population densities obtained during an MSMPR experiment vs. particle volume at two stirring times, for a stirring rate of 700 rpm.

This equation is relatively easy to solve if G_v is independent of size. In general, it is admitted that the linear growth rate is independent of size [17]. In the case of the crystallization of calcium sulphate hemihydrate, Mixed Suspension Mixed Product Removal (MSMPR) experiments showed that G_v was not size dependent. As an example of such experiments, Fig. 5 shows that the semilogarithmic representation of Ψ' as a function of the crystal volume, under conditions with negligible agglomeration, is a straight line except for very small crystals. Therefore, one can consider that G_v is a constant. We will return to this figure in the section describing the results.

3.2. Population balance related to volume densities

Since the volume growth rate is not size dependent, it is more convenient to write and to solve the balance equation related to volume population densities. In addition, when two particles of mass m_1 and volume u and mass $m-m_1$ and volume $v-u$ coalesce and form a single particle of volume v and mass m, there is conservation of both mass and volume. Therefore, this population balance is also appropriate for solving agglomeration problems, as obtained during the calcium sulphate hemihydrate crystallization process.

The population balance expressed with respect to the equivalent volume of the particles is, since G_v is not size dependent,

$$\frac{\partial \Psi'(t,v)}{\partial t} + G_v \frac{\partial \Psi'(t,v)}{\partial v} = r_{Av} \tag{8}$$

The boundary condition allowing the calculation of the nucleation rate B is given by:

$$B = \Psi'(t,0) G_v \tag{9}$$

In Eq. (8), r_{Av} is the distribution of the agglomeration rates, defined as the variation, per unit time, of the distribution of the particle number due to agglomeration. This distribution can be written as:

$$r_{Av} = k_e(A - D) \tag{10}$$

where A is the number of particles generated in class v by the collisions between particles of volumes u and $v-u$, per unit time and volume suspension. A is given by

$$A = \frac{1}{2}\int_0^v \Psi'(t,u)\,\Psi'(t,v-u)\,\mathrm{d}u \tag{11}$$

where the factor 1/2 takes the symmetry of the agglomeration phenomenon into account. D characterizes the disappearance of the particles from the same class v by agglomeration with other particles, and is given by

$$D = \Psi'(t,v)\int_0^\infty \Psi'(t,u)\,\mathrm{d}u \tag{12}$$

It is supposed here that k_e, the agglomeration kernel which provides information on the agglomeration rate of the particles of volume u and $v-u$, depends only on the particle environment but not on its shape and size.

The moment of order j of the population density function is

$$\mu_j = \int_0^\infty v^j \Psi'(t,v)\,\mathrm{d}v \tag{13}$$

Following the treatment by Hulburt and Katz [18] the transform of the population balance into moment is written as

$$\frac{\mathrm{d}\mu_j}{\mathrm{d}t} = G_v[j\mu_{j-1} - \Psi(t,v)v^j]_0^\infty + k_e\left\{\frac{1}{2}\left[\sum_{k=0}^{j}(C_k^j)\mu_k\mu_{j-k}\right] - \mu_k\mu_j\right\} \quad j=0,1,2\ldots \tag{14}$$

In this equation, the binomial coefficient is given by

$$(C_k^j) = \frac{j!}{k!(j-k)!} \tag{15}$$

Accordingly, the equations for the moments of orders 0, 1 and 2 are obtained as:

$$\frac{\mathrm{d}\mu_0}{\mathrm{d}t} = B - \frac{1}{2}k_e\mu_0^2 \tag{16}$$

$$\frac{\mathrm{d}\mu_1}{\mathrm{d}t} = G_v\mu_0 \tag{17}$$

$$\frac{\mathrm{d}\mu_2}{\mathrm{d}t} = 2G_v\mu_1 + k_e\mu_1^2 \tag{18}$$

from which it turns out that the volume growth rate G_v and the nucleation rate B are

$$G_v = \frac{\Delta\mu_1}{\bar{\mu}_0\Delta t} \tag{19}$$

$$B = \frac{\Delta\mu_0}{\Delta t} + \frac{1}{2}k_e\bar{\mu}_0^2 \tag{20a}$$

The agglomeration kernel, assumed to be independent of crystal habit and size, is calculated from Eq. (20), derived from Eq. (18):

$$k_e = \frac{\Delta \mu_2}{\Delta t \bar{\mu}_1^2} - \frac{2G_v}{\bar{\mu}_1} \quad (20b)$$

Over the time lag Δt, $\bar{\mu}_0$ and $\bar{\mu}_1$ are the mean values of μ_0 and μ_1. Values of k_e as a function of supersaturation and H_2SO_4 are given elsewhere [19].

The conversion of a population density, expressed as a function of the equivalent volume of the particles, into a population density expressed as a function of equivalent diameter is

$$\Psi(t,L)\mathrm{d}L = \Psi'(t,v)\mathrm{d}v \quad (21)$$

$$\Psi(t,L)\mathrm{d}L = 3\Psi'(t,v)fL^2\mathrm{d}L \quad (22a)$$

$$\Psi(t,L) = 3\Psi'(t,v)fL^2 \quad (22b)$$

where f is a shape factor of the particles. Particles are supposed to be spherical for the calculations.

The relation between linear and volume moments is obtained by inserting $\Psi'(t,v)$ of Eq. (22) in Eq. (13). The moment of order j, expressed in terms of equivalent diameters, becomes

$$\mu_j = \int_0^\infty v^j \Psi'(t,v)\mathrm{d}v = f^j \int_0^\infty \frac{L^{3j}\Psi(t,L)}{3fL^2}\mathrm{d}v \quad (23)$$

i.e.

$$\mu_j = f^j \int_0^\infty L^{3j}\Psi(t,L)\mathrm{d}L \quad (24)$$

Finally we get

$$\mu_j = \bar{\mu}_{3j} f^j \quad (25)$$

From here, G_v can be expressed and calculated as a function of the linear moments:

$$G_v = f\frac{\Delta \bar{\mu}_3}{\bar{\mu}_0 \Delta t} \quad (26)$$

4. Results

Fig. 6 gives an example of the evolution of the calcium concentration in a solution at 90 °C, 40% P_2O_5, with 2% H_2SO_4 excess and $\sigma_0 = 0.22$. As the crystallizer was not seeded, we observe three zones in the figure. Zone I represents the induction period for primary nucleation. Zone II corresponds to primary nucleation and growth. Zone III corresponds to growth and secondary nucleation.

Once primary nucleation has stopped, the consumption of the solute is mainly due to growth and to the production of new crystallites by secondary nucleation. These processes, which arise in Zones II and III, are analysed hereafter. In Table 1 we have reported the experimental conditions. All experiments, but no. 11 (for which the stirring rate was 300 rpm), were carried out with a stirring rate of 500 rpm.

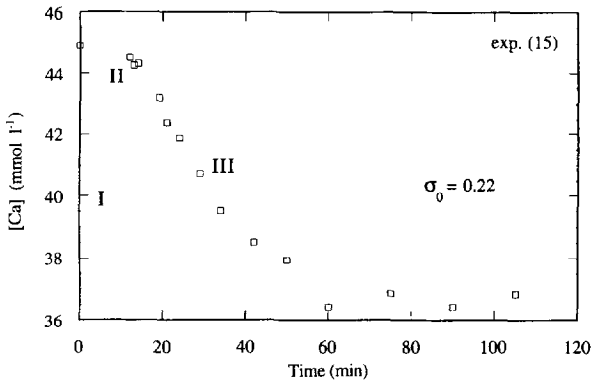

Fig. 6. Evolution of the calcium concentration during a batch crystallization.

Table 1
Initial supersaturations and H_2SO_4 excesses used during batch crystallizations carried out at 90 °C, 40% P_2O_5

Exp. no.	% H_2SO_4	σ_0
1	0.5	0.35
9	1	0.41
10	0.82	0.36
11	0.82	0.41
15	2	0.23
13	4	1.53
16	4	0.50
18	6	0.37

4.1. Effect of supersaturation

The bimodal character in the particle concentration (Fig. 3) and the existence of the inflexion point on the curve of the population density distribution (Fig. 4) are clear signs of the existence of agglomeration [20]. To demonstrate the influence of supersaturation on agglomeration, two experiments were carried out at 90 °C, 40% P_2O_5, 4% H_2SO_4 excess at initial supersaturations $\sigma_0 = 1.53$ (Fig. 7) and $\sigma_0 = 0.51$ (Fig. 8).

At $\sigma_0 = 1.53$ (Fig. 7), nucleation occurs immediately. After 3 min, the size distribution exhibits an inflexion point at about 25 μm (e.g. $v = 8200$ μm^3), which shows that agglomeration has already begun. At that time, supersaturation has dropped to $\sigma = 0.009$ and we may consider that the influence of growth is negligible. On the other hand, agglomeration takes place up to 6 min where we reach the maximum of the population density for the particles larger than 25 μm (e.g. $v = 8200$ μm^3). At 6 min, the number of particles smaller than 25 μm (e.g. $v = 8200$ μm^3) has considerably decreased, which indicates that agglomeration occurs between small and large crystals. In addition, the agglomerates are numerous and brittle when their size exceeds 25 μm. This is a consequence of the stirring rate (500 rpm) which

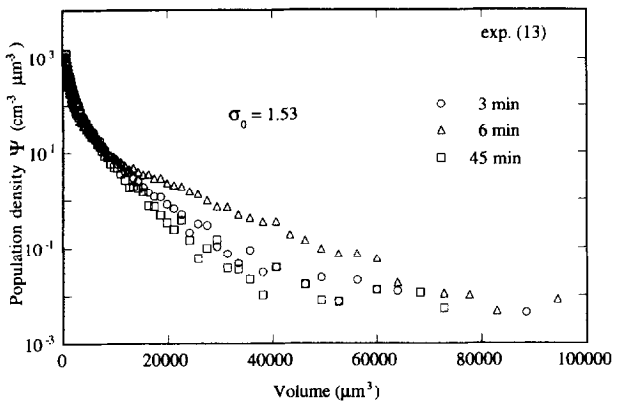

Fig. 7. Population densities at $\sigma_0 = 1.53$ vs. particle volume, at different crystallization times.

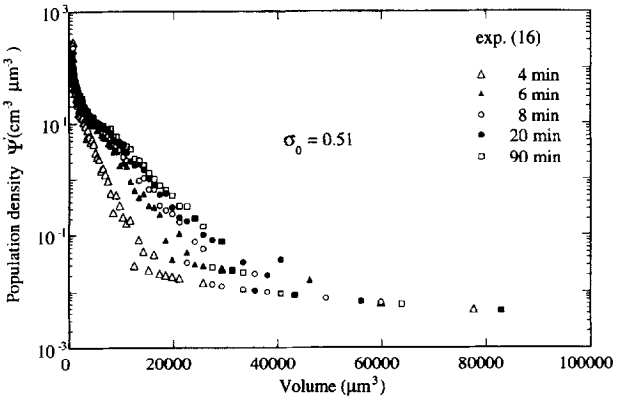

Fig. 8. Population densities at $\sigma_0 = 0.51$ vs. particle volume, at different crystallization times.

breaks the agglomerates, and we can see from Fig. 7 that after 45 min, stirring has completely destroyed the agglomerates formed before.

At $\sigma = 0.51$ (Fig. 8) the size of the agglomerates always increases and no breakage is observed. The population density distributions exhibit inflexion points for the sizes ranging from 14.5 to 25 µm (e.g. volumes ranging from 1600 to 8200 µm^3), showing that agglomeration also occurs between small and large particles.

4.2. Effect of breakage

To verify our hypothesis of a constant volumic growth rate G_v, and to come closer to industrial process conditions, continuous operations in a MSMPR crystallizer have been carried out. Fig. 5 shows the result of such an experiment under steady state conditions. The obtained population density is presented in a semilogarithmic diagram as a function of the crystal volume: except for the smallest crystals we get a straight line. Since agglomeration is not very efficient under the conditions of this experiment, one can assume that G_v is not a function of crystal volume. On the other hand, the crystals in suspension (22.8 g in 1 l of saturated solution) have been stirred over a long time in the batch vessel under high stirring rates (700 rpm). The population density curve

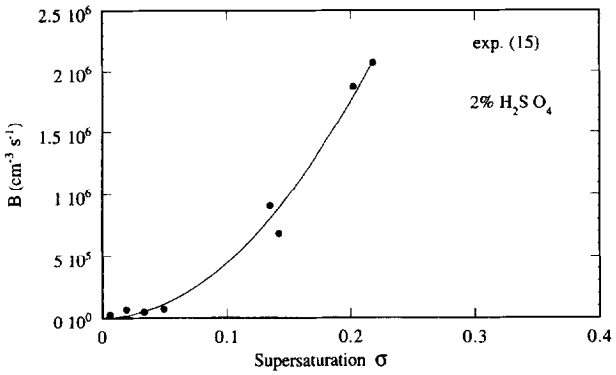

Fig. 9. Nucleation rates B of calcium sulphate hemihydrate vs. supersaturation.

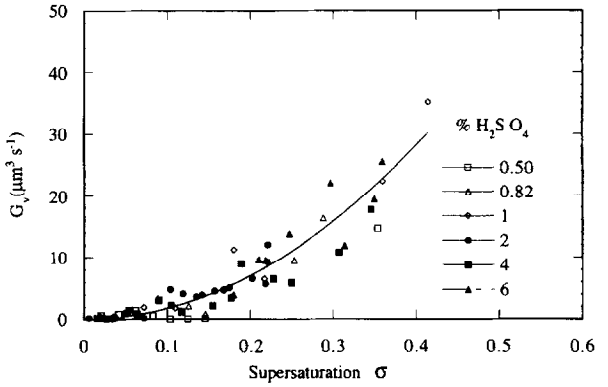

Fig. 10. Variation of the overall volume growth rate G_v vs. supersaturation, for different H_2SO_4 excesses.

we obtained after 2 h can be superimposed on the initial curve. This demonstrates pretty well that hemihydrate crystals are not broken even at high stirring rates. On the contrary, dihydrate particles suffer attrition depending on the residence time in the crystallizer [21].

4.3. Nucleation and growth rates

The integral given in Eq. (13) can be calculated by a computer after discretization of all class sizes of the distribution:

$$\mu_j(t,v) = \sum_{i=1}^{n} \frac{v^j \psi(t,v_i) + v^j \psi(t,v_{i-1})}{2} \times \Delta v_i \qquad (27)$$

Moreover, using the moments method it was possible to estimate B and G_v. Fig. 9 shows the evolution of the nucleation rate B with supersaturation. The volume growth rates G_v versus supersaturation are displayed in Fig. 10.

4.4. Effect of H_2SO_4 excesses

Sulphuric acid plays an essential role in the crystallization process of hemihydrate. That is the reason why we paid special attention to this parameter.

Table 2
Kinetic coefficients of the nucleation rates calculated by the moments method, for different H_2SO_4 excesses

% H_2SO_4	$k' \times 10^{-6}$ cm^{-3} s^{-1}
0.50	8
0.82	2
1	8.7
2	39.6
4	6.7
6	–

4.4.1. Influence on growth rates

Figs. 9 and 10 show that nucleation and growth rates are quadratic functions of supersaturation, even if we note that there is some dispersion of the experimental results. This latter point is not surprising for the system we are studying and a previous study [22] showed similar dispersions. In our opinion, dispersion results both from the material itself and from the needle-like shape of the crystals, which is not very favourable for size distribution measurements. This is also the reason why we decided to treat the experimental data using the moments method. The method, which consists of measuring the mean growth rate $\bar{G}_v = d\bar{v}/dt$ by following the evolution of the mean overall size $\bar{L}$, gives too much uncertainty because it does not give any insight into the different size classes. It is noteworthy that the H_2SO_4 excess affects the solubility curve (Fig. 2) and consequently the supersaturation, too, but that has no significant effect on the hemihydrate growth rate. If there is an effect, it is hidden within the scattering of the experimental points.

As far as the volume growth rate G_v (Fig. 10) is concerned, it can be written as $G_v = k_v\sigma^2$ with $k_v = 175.5$ μm^3 s^{-1}.

4.4.2. Influence on nucleation rate

The experiments in which the H_2SO_4 excess ranged from 0.5% to 6% show that B is also a quadratic function of supersaturation: $B = k'\sigma^2$. However, no nucleation is observed below a certain threshold ranging from $\sigma = 0.1$ to $\sigma = 0.05$ with increasing H_2SO_4 excess. At 2% (Fig. 9) nucleation is important with $k' = 3.9 \times 10^7$ cm^{-3} s^{-1}. This value, the highest we obtained, shows that homogeneous nucleation takes place even at low supersaturation. Beyond 2% H_2SO_4 excess, the nucleation rate decreases as shown in Table 2. This clearly shows that the nucleation mechanism itself is a function of sulphuric acid excess.

4.5. Effect of stirring rate

The experiments carried out with stirring rates of 500 and 300 rpm (nos. 10 and 11 respectively in Table 1), all other parameters being constant, give similar values of the nucleation rates. Both curves $B = k'\sigma^2$ coincide, having about the same kinetic coefficient $k' = 2 \times 10^6$ cm^{-3} s^{-1} beyond $\sigma = 0.1$ (Fig. 11).

On the other hand, growth rates are slightly affected by the stirring rate, the crystals growing only a little more rapidly at

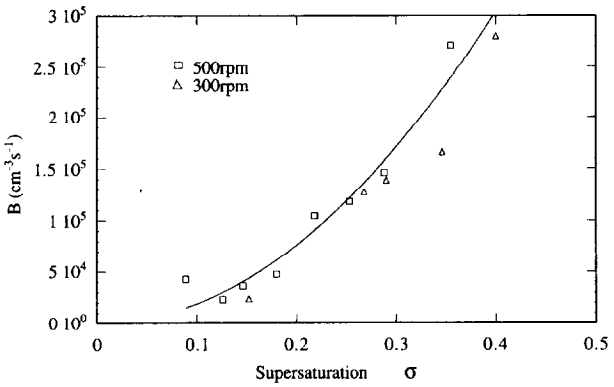

Fig. 11. Influence of the stirring rate on the nucleation rate B.

500 rpm than at 300 rpm. It appears that mass transfer slightly influences the crystal growth.

5. Conclusion

Crystallites of calcium sulphate hemihydrate were obtained by primary nucleation at 90 °C in a batch crystallizer, the aqueous solution containing phosphoric acid (40% P_2O_5) and sulphuric acid excess up to 6%. Supersaturation with respect to hemihydrate was adjusted at different values up to 50%. Primary nuclei grow and give crystals, which generate new nuclei by secondary nucleation. Primary nucleation was especially important when the H_2SO_4 excess was 2%.

The evolution of the population density was followed by removal of homogeneous samples of the suspension. The population balance was estimated by means of the moments method, taking into account that agglomeration is important. From the different treatments it turned out that the hemihydrate growth rates are quadratic functions of supersaturation. These growth rates are influenced by H_2SO_4, but only because it affects the hemihydrate solubility and consequently supersaturation. On the other hand, the nucleation rates are significantly influenced by H_2SO_4 itself, being also quadratic functions of supersaturation. The highest nucleation rate was obtained with 2% H_2SO_4 excess, probably because homogeneous nucleation is superimposed on heterogeneous and secondary nucleation. It is noteworthy that in industrial plants, the loss of P_2O_5 trapped into or onto the crystals is the lowest (0.2%) just for this H_2SO_4 excess. In our solutions, agglomeration is also the lowest at 2% H_2SO_4 excess [19]. However, we have not found any simple physico-chemical reason for explaining this point. We only note that an excess of 2% H_2SO_4 reduces agglomeration, which in turn reduces the amount of P_2O_5 trapped by the hemihydrate crystals.

According to our study, the moments method provides a good estimation of the kinetic parameters for nucleation and growth of calcium sulphate hemihydrate crystals in concentrated phosphoric acid solutions. This is due to the fact that this method takes agglomeration into account. The agglomerates formed at high supersaturation are more brittle than those formed at low supersaturation. This is probably due to

crystal elongation, which rapidly increases with increasing growth rates, i.e. with increasing supersaturation.

Appendix A. Notation

A	number of particles generated by agglomeration in a size class (number $cm^{-3} s^{-1}$)
B	nucleation rate (number $cm^{-3} s^{-1}$)
C, C_0	actual concentration and solubility (mol m^{-3})
D	number of particles disappearing by agglomeration from a size class (number $cm^{-3} s^{-1}$)
G	growth rate ($\mu m^3 s^{-1}$)
L_i	equivalent diameter of the particles in the size class i (μm)
k	kinetic coefficient of growth rate ($\mu m^3 s^{-1}$)
k'	kinetic coefficient of nucleation rate (number $cm^{-3} s^{-1}$)
r_A, r_B	distribution of agglomeration and breakage rates (number $cm^{-3} \mu m^{-3} s^{-1}$)
$[N]$	concentration of particles in suspension (number cm^{-3})
v	particle volume (μm^3)
Δv	width of a size class (μm^3)
$\Psi(L)$	number of crystals per unit volume of suspension and width in the size class L (number $cm^{-3} \mu m^{-1}$)
$\Psi'(v)$	number of crystals per unit volume of suspension and width in the volume class v (number $cm^{-3} \mu m^{-3}$)
σ	supersaturation $(C - C_0)/C_0$
μ_j	moment of order $j = 1$, 2 or 3 of the population density function

References

[1] E.T. White, S. Mukhopadhyay, Crystallisation of gypsum from phosphoric acid solution, Am. Chem. Soc. Symposium Series 438 (1990) 291–315.

[2] M.E. Pozin, B.A. Kopylev, V.L. Varshavski, L. Pinto, Crystallization of calcium sulphate during the interaction of monocalcium phosphate with sulphuric acid in phosphorique acid, Zh. Prikl. Khimii 34 (11) (1961) 2261–2265.

[3] S.E. Dahlgren, Physico-chemical background of phosphoric acid manufacture by wet processes, Acta Phys. 271 (1960) 3–15.

[4] N.S. Torocheshnikov, I.A. Petrovlovskii, Continuous recrystallization of calcium sulfate dihydrate to the hemihydrate in the phosphoric acid wet process, Zh. Prikl. Khimii 59 (6) (1986) 1201–1205.

[5] J. Frochen, J. Lainé, H. Allyot, G. Gosse, Procédé de fabrication d'acide concentré par double cristallisation, Inf. Chimie 118 (1973) 105–118.

[6] V.F. Karmyshov, G.S. Bochkarev, B.I. Shub, E.V. Khlebodarova, S.Ya. Shpunt, Hemihydrate method for production of concentrated phosphoric acid..., Zh. Prikl. Khimii 48 (11) (1975) 2345–2347.

[7] V.V. Godobole, Proc. Lecture Series on 'Recent Advances in Inorganic Acid Industry', Indian Chemical Manufacturing Association, Bombay, 1980.

[8] A.B. Amin, M.A. Larson, Crystallization of calcium sulfate from phosphoric acid, Ind. Eng. Chem. Proc. D. D. 7 (1) (1968) 133–137.

[9] F. Gioia, G. Mura, A. Viola, Analysis, simulation, and optimisation of the hemihydrate process for the production of phosphoric acid from calcareous phosphorites, Ind. Eng. Chem. Proc. D. D. 16 (3) (1977) 390–399.

[10] J.E. Davenport, J.G. Getsinger, F. Carrol, Wet-process phosphoric acid foam distribution of sulphuric acid, Ind. Eng. Chem. Proc. D. D. 4 (1) (1965) 84–88.

[11] S. van der Sluis, G.J. Witkamp, G.M. van Rosmalen, Crystallization of calcium sulfate in concentrated phosphoric acid, J. Cryst. Growth 79 (1986) 620–629.

[12] J.C. Masy, M. Cournil, Using a turbidimetric method to study the kinetics of agglomeration of potassium sulphate in a liquid medium, Chem. Eng. Sci. 46 (1991) 693–701.

[13] P. Marchal, R. David, J.P. Klein, J. Villermaux, Crystallization and precipitation engineering I: an efficient method for solving population balance in crystallization with agglomeration, Chem. Eng. Sci. 43 (1) (1988) 59–67.

[14] M. Jansen, A. Wallen, J. Verbiest, R.C. Van Lands Shout, G.M. van Rosmalen, Incorporation of phosphoric acid in calcium sulfate hemihydrate from a phosphoric acid process, in: S.J. Jancic, E.J. de Jong (Eds.), Industrial Crystallization, Elsevier Science, Amsterdam, 1984, pp. 171–176.

[15] J.M. Sullivan, J.J. Kohler, J.H. Grinstead, Solubility of α-calcium sulfate hemihydrate in 40, 50 and 55% P_2O_5 phosphoric acid solution at 80, 90, 100, and 110 °C, J. Chem. Eng. Data 33 (1988) 367–370.

[16] S. Khan, Master of studies project report, University of Queensland, 1986.

[17] W.L. McCabe, Ind. Eng. Chem. 21 (1929) 30–33.

[18] H.M. Hulburt, S. Katz, Some problems in particle technology: a statistical mechanical formulation, Chem. Eng. Sci. 19 (1964) 555–574.

[19] M. El Moussaouiti, R. Boistelle, A. Bouhaouss, J.P. Klein, Agglomeration kinetics of calcium sulphate hemihydrate crystals in sulpho-phosphoric solutions, J. Cryst. Growth 169 (1996) 118–123.

[20] J.R. Bechman, R.W. Farmer, Bimodal CSD barite due to agglomeration in an MSMPR crystallizer, AIChE Symp. Ser. 83 (253) (1987) 85–94.

[21] J. Nyvlt, S. Zacek, Batch crystallisation with crystals attrition, Collect. Czech. Chem. C. 58 (1993) 1855–1859.

[22] P. Karpinski, K. Toyokura, Secondary nucleation and growth of copper sulphate crystals in a fluidized bed, in: E.J. de Jong, S.J. Jancic (Eds.), Industrial Crystallization, 1978, pp. 55–64.